POWER-FREQUENCY INTERACTIONS IN AN AC/DC/AC SYSTEM

A Thesis Submitted to

The Faculty of Graduate Studies

in Partial Fulfilment of the Requirements for

the Degree of Master of Science

in the Department of

Electrical Engineering

University of Saskatchewan

by

Murray Gordon Bennett

Saskatoon, Saskatchewan

January 1976

ACKNOWLEDGEMENTS

The author expresses his gratitude to Dr. Mohindar S. Sachdev for helpful advice and assistance during the course of this project and preparation of this thesis. As well, he wishes to thank Mr. Horst E. Wichert and the engineers of the System Planning Department of Manitoba Hydro for providing system data.

Thanks are also due to the University of Saskatchewan for the scholarship received during the later portion of the project. Part of this work was financed by the National Research Council of Canada grant No. A7249.

UNIVERSITY OF SASKATCHEWAN

Electrical Engineering Abstract 76A174

"POWER-FREQUENCY INTERACTIONS
IN AN AC/DC/AC SYSTEM"

Student: M.G. Bennett Supervisor: Dr. M.S. Sachdev

M.Sc. Thesis presented to the College of Graduate Studies

January 1976

ABSTRACT

A study of power-frequency interactions in an AC/DC/AC system is presented in this thesis. The selected system consists of three connected hydro-electric generating stations, which transmit power to a receiving AC system over two HVDC bipolar transmission links. Mathematical models of the DC bipoles, and the sending end and receiving end AC systems are developed and are amalgamated to provide an equivalent of the composite AC/DC/AC system. The derived linearized model is suitable for representing low frequency power-frequency interactions.

The model of the DC bipole includes representation of the firing angle, master current order and power order controllers. The sending end generators are represented by voltages behind transient reactances and inertial equations. The voltages behind the transient reactances are assumed to vary such that voltages at the high tension buses are maintained constant. To concentrate on interactions between the sending end generators and the DC bipoles, the receiving end system is assumed to be an infinite bus.

The stability of the composite AC/DC/AC system is investigated using root locus studies and real time simulations. The sending end system is unstable when the DC links are operated in the constant power mode. It is shown that modulation of power flow of the DC links stabilizes the system. Lead-lag and double lead-lag modulators are investigated.

TABLE OF CONTENTS

LIST OF FIGURES

LIST OF TABLES

CHAPTER 1

INTRODUCTION

The hydro electric potential of the Nelson River in Northern Manitoba has been estimated to be greater than 7000 MW.[1] At the first stage of development, Kettle Rapids generating station was constructed on the Nelson River. A bipolar HVDC transmission link was erected to transmit the electrical energy from Kettle Rapids to Winnipeg, a distance of 550 miles.[2] In the next phase of development, two additional plants will be built; one at Long Spruce and the other at Limestone. Another bipolar DC link will be constructed to transmit power from Limestone to Winnipeg.

At the northern end, Kettle Rapids, Long Spruce and Limestone plants will be interconnected by 230 kV transmission lines. Three 12.8 mile long AC lines will connect Kettle Rapids to Long Spruce. A similar arrangement will be used between Long Spruce and Limestone. The voltage at the Kettle Rapids high tension bus is 138 kV; therefore, three 138/230 kV auto-transformers will connect the Kettle switchyard to the 230 kV system. The three generating stations at the sending end are similar. Each plant will ultimately consist of 10 hydro-turbine generator sets, each of 102 MW (120MVA) capacity; therefore, the total installed capacity at each station will be 1020 MW.

Many studies of the first Nelson River HVDC link (bipole I) have been reported in the literature.[1,2,3,4] This bipole has a nominal rating of ±450 kV and 1800 amps. At the time of constructing this bipole, two parallel HVDC transmission lines were erected. One of these lines will now be used

for the second bipole which will have a nominal rating of ±500 kV and 2000 amps. One of the DC transmission lines will be extended to the Limestone station. Both DC links will feed their respective inverter stations at Dorsey, near Winnipeg. A single line diagram of this system is shown in Figure 1.1. It should be noted that this system is at an intermediate point of development and at this stage the installed DC transmission capability exceeds the generation capacity by approximately 600 MW.

1.1 Dynamic Stability

In normal operation small frequency deviations are experienced continuously. These oscillations are associated with changes in generator outputs, bus voltages, line flows and system loads. In general, these oscillations can be divided into two groups[3]: oscillations with a frequency range of 0.01 to 0.20 Hz, usually associated with governors; and oscillations in the range of 0.2 to about 3 Hz, associated with exchanges of power between generating plants in the system. In many cases, power-frequency oscillations between generating plants may be underdamped.

It has been demonstrated in the past[3,4,5,6] that modulation of power flow on HVDC links can improve the damping of oscillations on the AC system. This thesis investigates the use of power modulation of the DC links to improve dynamic stability of the Nelson River generating system as described above.

1.2 HVDC Power Modulation

Power modulators have been used on commercial HVDC schemes, notably; the Nelson River bipole I[3,4]; the Pacific Northwest-Southwest intertie[5]

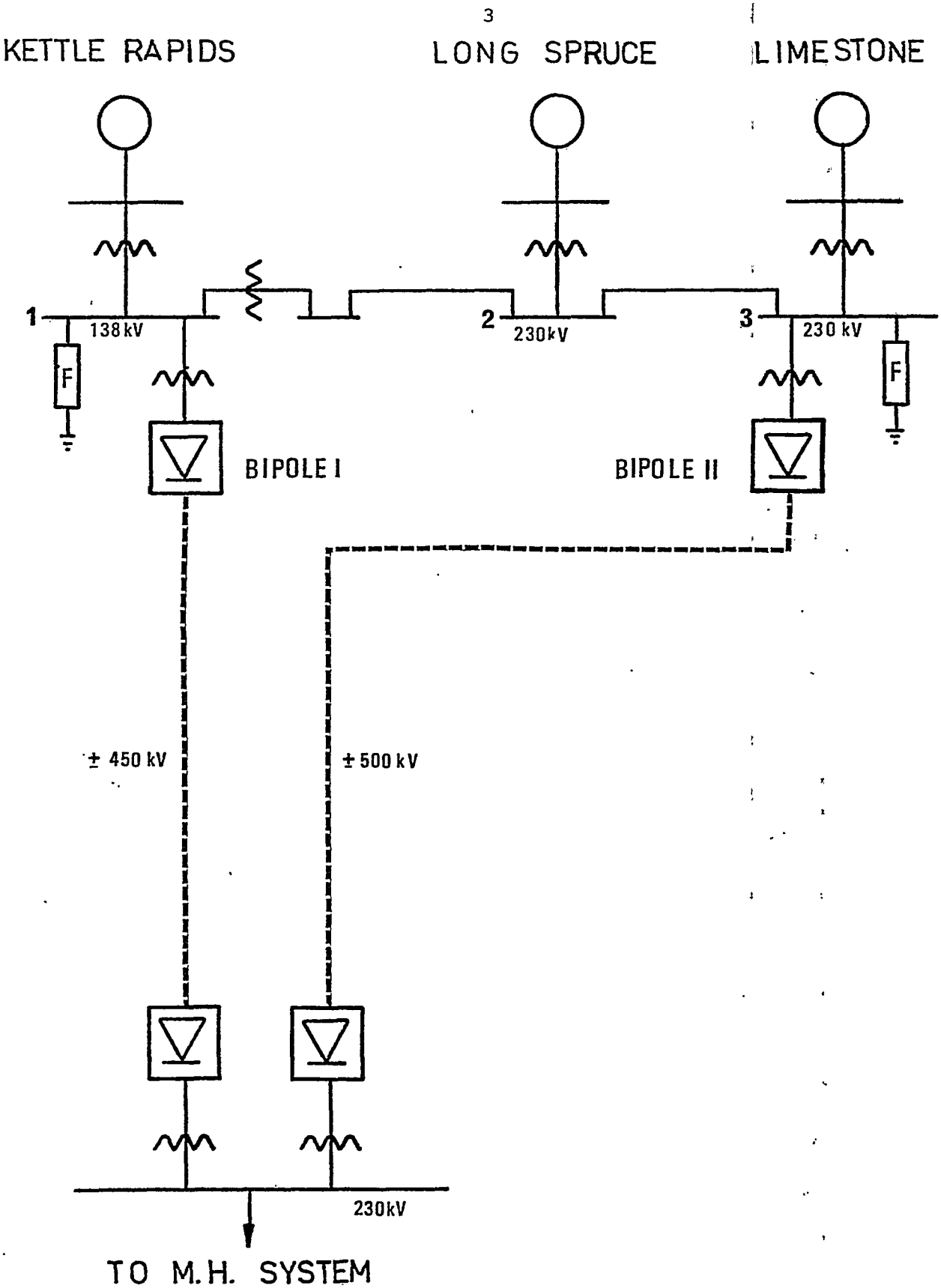

Figure 1.1 Single line diagram of the AC/DC/AC system

and the Eel River[6] scheme. Different approaches were used to design the power modulators for these projects. Hamlin and Roche[3] used a reduced linearized system model on an analogue computer for preliminary design. The design of the modulator was then finalized by real time simulations on an Electrical Network Analogue. Cresap and Mittlestadt[5] selected a power modulator for the Pacific intertie from system studies using a modified transient stability program. Paterson[6] et.al. used a linearized system model for the preliminary design of the controller. However, the ultimate selection of the modulator was based on system performance in the time domain.

Different levels of complexity can be used to derive mathematical models suitable for investigating power-frequency interactions between AC and DC systems. In this thesis, a simplified mathematical model of the AC/DC/AC system, shown in Figure 1.1, has been developed. A model of this nature serves to highlight some of the important power-frequency interactions of less than 3 Hz frequency. The order of this model is very small compared to that of a complete equivalent. This simplified approach has been used for investigating the power-frequency oscillations and for preliminary design of the power modulators. This method provides a "feel" for the expected modes of oscillation, which can assist in subsequent studies using a more detailed representation of the system.

The approach adopted during this work was to derive models of the subsystems, (i.e. the DC bipoles; the sending end and the receiving end AC systems) and combine them to obtain a system equivalent. Before developing the models of the subsystems, a general background of HVDC transmission is presented in Chapter 2. Following this, a linearized model of a bipolar HVDC link is developed in Chapter 3. This model of the DC link

includes representations of the firing angle, current order and power order controllers. In Chapter 4, linearized models of the sending and receiving end AC systems are derived. These models are valid for power-frequency interactions of frequencies less than 3 Hz. The AC and DC representations are amalgamated into a complete model of the AC/DC/AC system in Chapter 5. Two power modulators are designed in Chapter 6. The dynamic stability of the system equipped with the proposed modulators has also been examined using the root locus technique and small signal simulations. The results of these studies are presented in Chapter 6.

CHAPTER 2

BACKGROUND OF HVDC TRANSMISSION

As outlined in the previous chapter, the objective of this project is to study the power-frequency interactions of an AC/DC/AC system. Before a suitable model of the DC system is developed, background of DC transmission is briefly reviewed for ready reference of the reader.

HVDC transmission has been proven feasible from the technical and economic standpoint. In many cases DC links have been preferred over AC interties, for example, the Pacific Northwest-Southwest intertie, the Eel River scheme and the Nelson River project. The advantages of HVDC transmission have already been well documented in the literature.[7,8,9] Some of these advantages are: no reactive voltage drop in transmission; asynchronous operation of the interconnected systems; controllability of power flow, etc. HVDC transmission has a few disadvantages also, such as: converters absorb reactive power; converters inject harmonics into the connected AC and DC systems, etc.

The basic unit in a modern HVDC system is the controlled three phase bridge converter shown in Figure 2.1. Under proper control, this device can be used to convert alternating voltage and current to direct voltage and current and vice versa. A bridge converter consists of six valves; each valve conducts once every AC cycle. Therefore, a converter of this type is called a six pulse bridge. It is possible to connect two identical bridges in series and use three phase AC voltages displaced by 30 electrical degrees to excite the two converters. This arrangement provides twelve pulse operation. Connecting the bridges in series doubles the DC voltage while

the current rating remains unchanged. From the AC side, two converters connected in this manner appear to be operating in parallel.

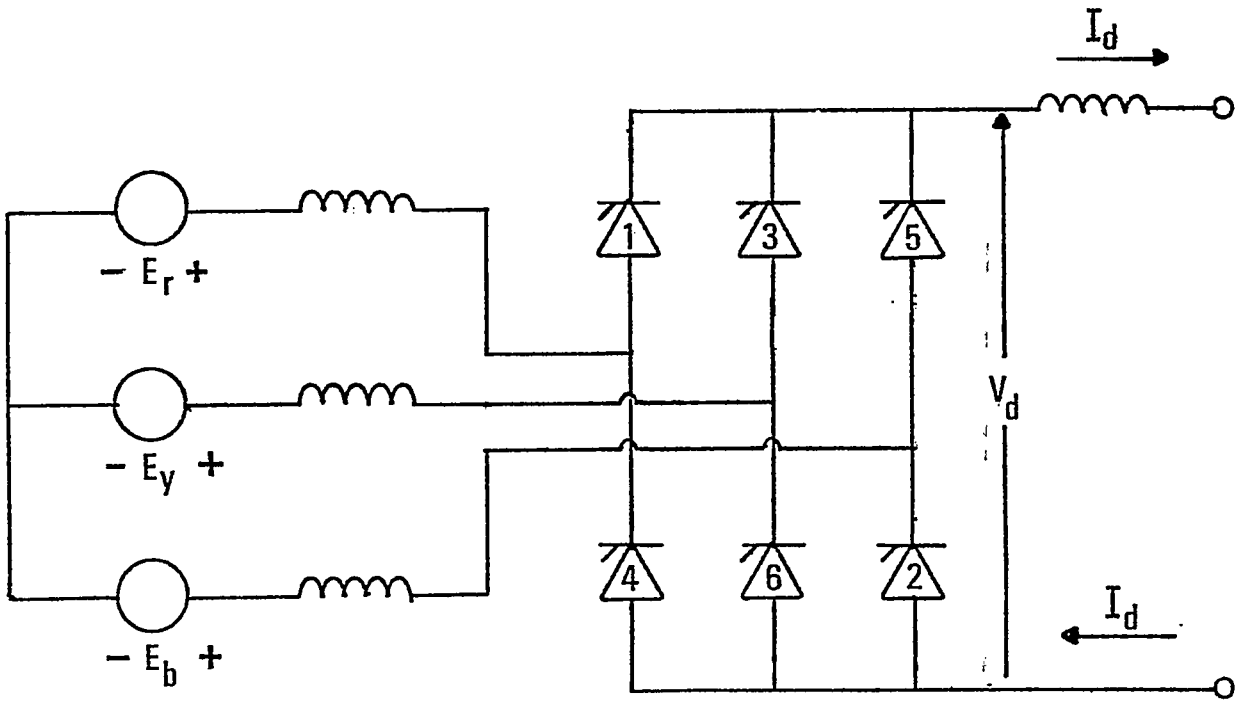

Figure 2.1 A typical six pulse bridge converter

A bipolar AC/DC/AC transmission system is shown in Figure 2.2. In this circuit, power is flowing from converter 1 to converter 2. Because the current, in the valves, can only flow in one direction, power flow in this transmission system can be reversed only by changing the polarity of DC voltage at each converter.

The series inductors, shown in Figure 2.2, attempt to maintain direct current flow. Typically, inductors of 0.4 to 2.0 Henries are used for this purpose. Other major components of a DC link include the AC and DC side

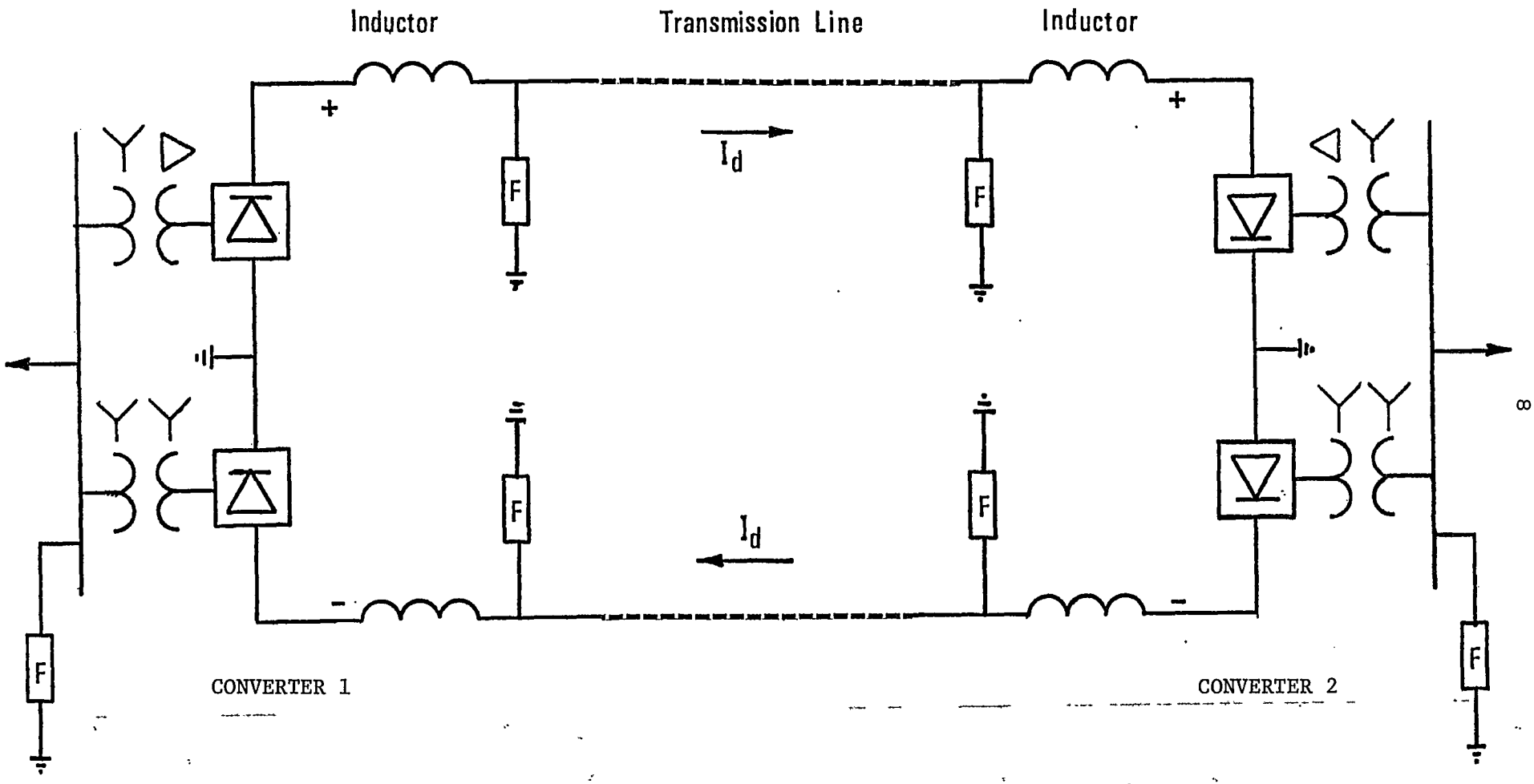

Figure 2.2 A typical bipolar DC scheme

filters, converter transformers and synchronous condensers. The AC and DC side filters divert most of the harmonics, generated by converters, away from the AC and DC systems. A converter transformer isolates the AC system from the DC side. Synchronous condensers and AC side filters provide the required reactive power.

2.1 Steady State Converter Characteristics

The output voltage of a converter, the essential components of which have been described above, is controlled by delaying the firing of each valve by an angle, say α, from the instants of natural conduction. Increasing the delay angle from 0° to about 90° progressively reduces the DC voltage output from a maximum value to zero. Over this range, power flows from the AC system to the DC. In this mode of operation, the converter is called a rectifier. Advancing the delay angle beyond 90 electrical degrees reverses the polarity of the direct voltage. Power now flows from the DC side to the AC system. In this mode, the converter is referred to as an inverter. In most rectifiers the delay angle is not reduced below a minimum permissible value of approximately 5°. Similarly, at the inverter, the extinction angle is not permitted to fall below a minimum value, say 7° to 20°.

2.1.1 Converter voltage equations

Equations describing the steady state operation of AC/DC converters are documented in the literature.[7,8,9] To facilitate the analysis, converter voltage equations are usually derived using the following assumptions[8]:

i) the resistance of transformers is negligible;

ii) AC side filters are ideal;

iii) direct current is constant and does not contain any harmonic components;

iv) the AC voltages are balanced;

v) the arc drops in the valves are negligable.

The direct voltage outputs of a multibridge rectifier and a multibridge inverter can be expressed as:

$$V_{dr} = N_B T_r U_{dro} \cos \alpha_r - \frac{3N_B w_r L_r}{\pi} I_d \qquad (2.1)$$

$$V_{di} = N_B T_i U_{dio} \cos \beta_i + \frac{3N_B w_i L_i}{\pi} I_d \qquad (2.2)$$

Where:

V_d is direct voltage;

I_d direct current;

U_{do} no load direct voltage per bridge;

L commutation inductance per bridge;

w nominal AC side frequency;

N_B the number of bridges in series;

T the transformer tap setting;

α firing delay angle;

β firing advance angle; and the

subscripts r and i denote rectifier and inverter respectively.

2.1.2 Converter control characteristics

The operational characteristics of a converter bridge can be shown conveniently on a V-I graph. Figure 2.3 shows the steady state characteristics of two converters connected back-to-back. Three modes of converter control, indicated in this figure, are: (1) constant delay angle, (2) constant current and (3) constant extinction angle controls. The intersection of the characteristics of two converters indicates the point of stable operation. For example, in Figure 2.3 the operating point shows that converter 1 is a rectifier under constant current control and converter 2 is an inverter under constant extinction angle control.

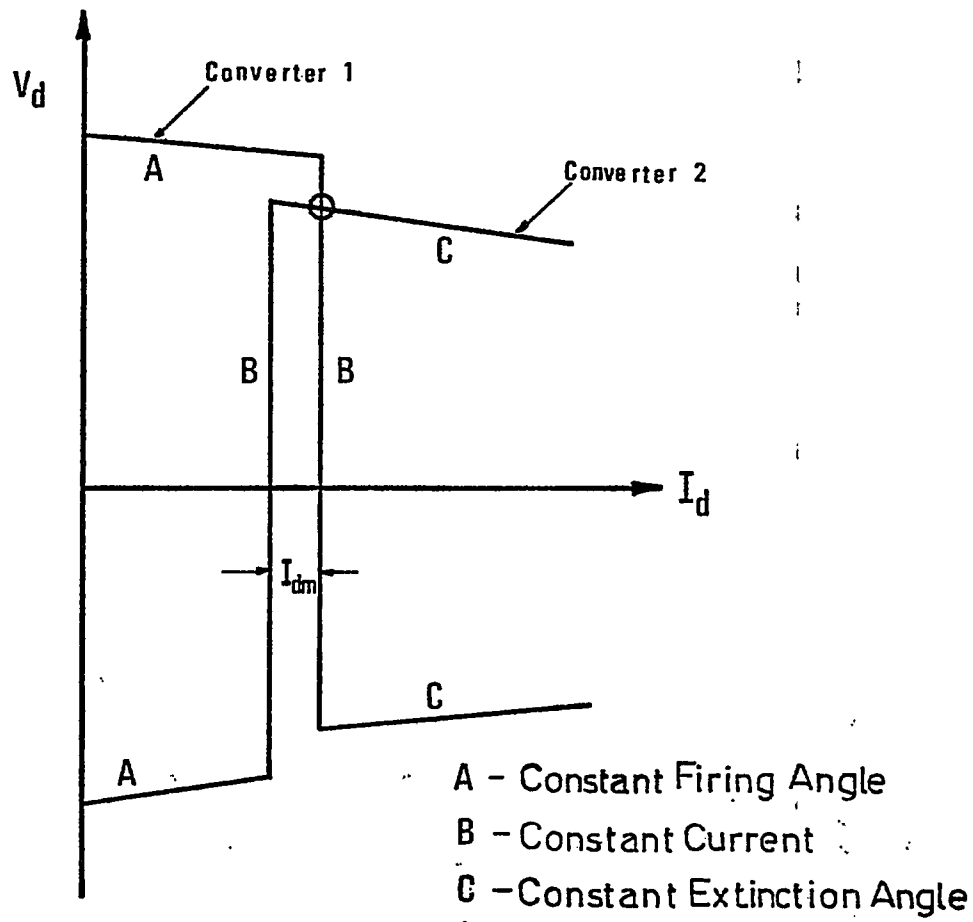

Figure 2.3 Control characteristics of two AC/DC converters

The difference between the current orders of the two converters is called the current margin. This margin is generally 10 to 15% of the operating current. In practice, equal current settings are provided at the rectifier and inverter and the current margin is subtracted from the setting at the inverter terminal.

2.2 Firing Angle Control

To ensure that a converter operates in the manner described in Section 2.1, the firing of its valves must be controlled. For this purpose, two main approaches are being used at present, namely: individual phase control and equidistant pulse control. In the former approach, all valves are fired at equal firing delays. Whereas, in the equidistant pulse control, valves are triggered at equal intervals of time.

2.2.1 Individual phase control

In individual phase control, each valve has a separate firing angle computer. In steady state, each valve is fired at a prespecified delay angle. Many designs for individual phase control have been developed in the past.[10,11,12] These controllers are suitable for both rectifier and inverter terminals. For illustration, one such control is described below.

The controller described in Reference 12 was designed for constant extinction angle (CEA) control, which is the most important mode of inverter operation. In this control, the valve commutation equation is simulated by the firing angle computer. For each valve, this equation can be expressed as:

$$e = -\sqrt{2}E \cos wt - \sqrt{2}E \cos \delta_c + 2wL I_d \qquad (2.3)$$

where: E is the valve side no load AC voltage and

δ_c is the extinction angle.

The valve is fired when e is zero and is changing from negative to positive. In this manner, the firing is advanced sufficiently to ensure that the desired extinction margin is maintained. The first two terms are generated by integrating the commutation voltage of the valve, as shown in Equation 2.4.

$$\int_{-\pi + \delta_c}^{wt} \sqrt{2}\, E \sin wt\, d(wt) = -\sqrt{2}\, E \cos wt - \sqrt{2}\, E \cos \delta_c \qquad (2.4)$$

At the negative-going zero of the commutation voltage, output of the integrator is clamped to zero for a small duration equal to δ_c after which the integration process for the next firing starts. The last term of Equation 2.3, $2wL\, I_d$, is realized as a voltage drop in a potentiometer set at resistance equal to 2wL with current I_d flowing in it. The output of the CEA controller is shown in Figure 2.4.

For constant current control, an additional voltage proportional to current error is added to the output of the CEA control computer. A minimum firing angle is assured by adding a negative pulse of width α_{min}, at the instant of natural commutation. A block diagram of this controller is shown in Figure 2.5.

2.2.2 Equidistant firing pulses

In steady state, an equidistant firing control pulses valves at equal intervals of time. Since the voltages of an AC system are not always balanced, the firing delays of all valves are not equal. Out of the controllers of this type presented in the literature[11,13,14], the equidistant firing control developed by ASEA[13] is described here.

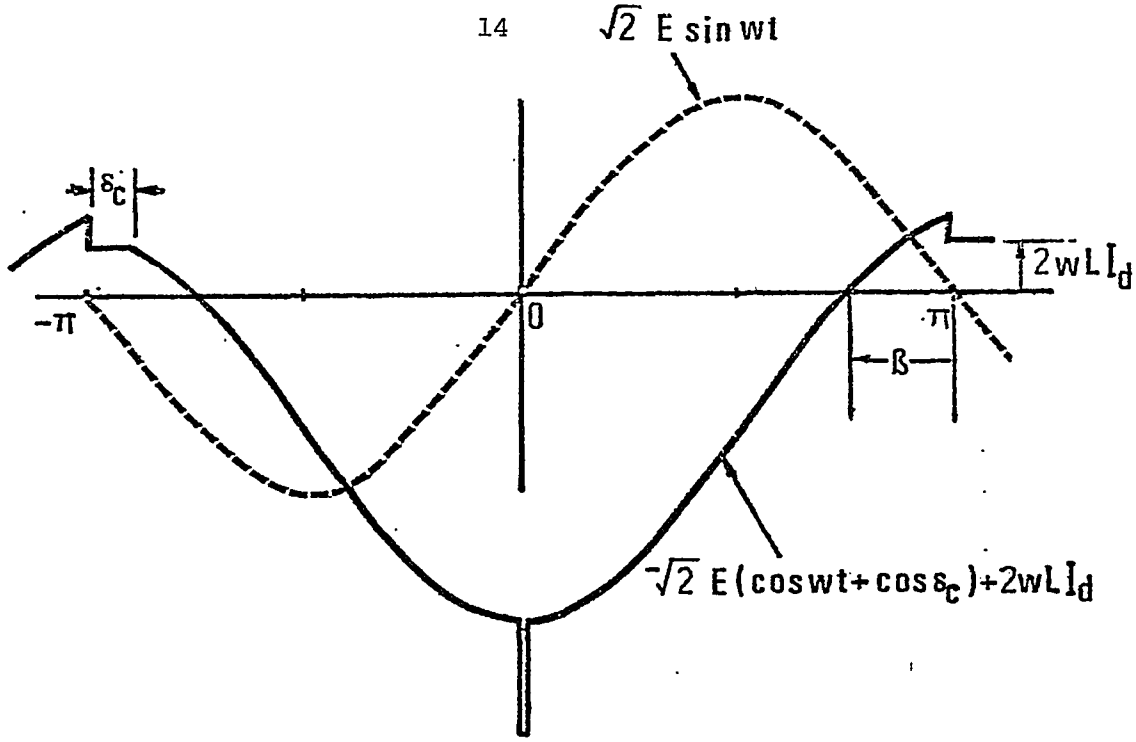

Figure 2.4 Input and output waveforms of a CEA controller

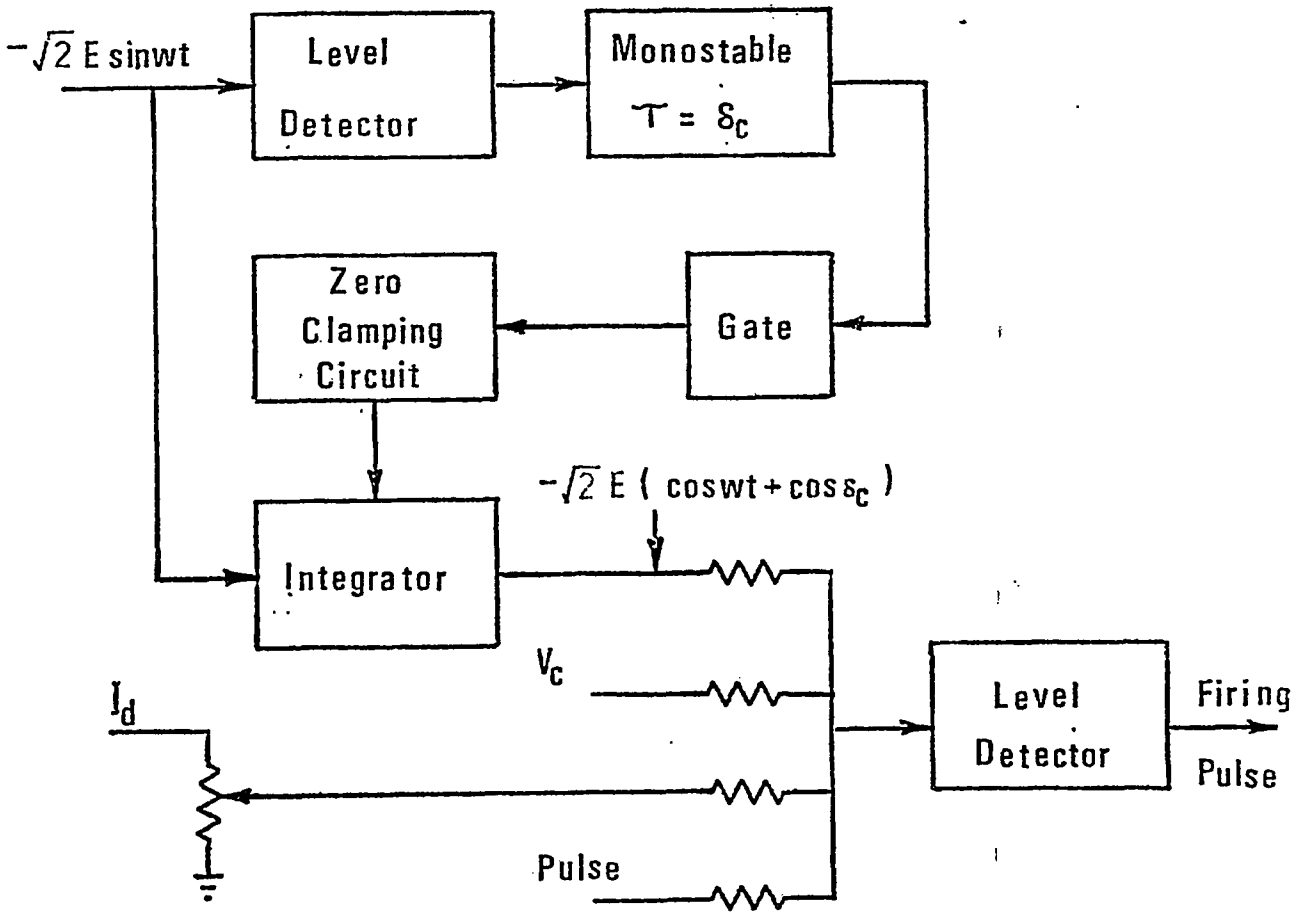

Figure 2.5 Block diagram of the valve firing angle controller

The heart of the firing angle control is a voltage controlled oscillator which, under steady state conditions, generates pulses at a frequency six times that of the AC system. The pulses from the oscillator drive a 6 stage ring counter which advances a "1" each time a pulse is received. The outputs from the ring counter are passed to the valve grids via a series of logical OR gates, producing pulses of 120° duration.

The voltage which controls the oscillator is made up of three components: a voltage proportional to the AC system frequency; constant current controller output proportional to the current error and a voltage from the CEA controller. A simplified block diagram of this controller is shown in Figure 2.6. Normally, the output of the current controller is zero. For a change in direct current, I_d, the error is amplified and thus the output, U_c, attains a value other than zero. The frequency of the pulses changes which advances or retards the valve firing angles. A step change in the oscillator input voltage changes the interpulse time and therefore the oscillator circuit acts as an inherent integrator.

A brief background of HVDC transmission has been presented in this chapter. The steady state equations and some modes of operation of AC/DC converters have been discussed.

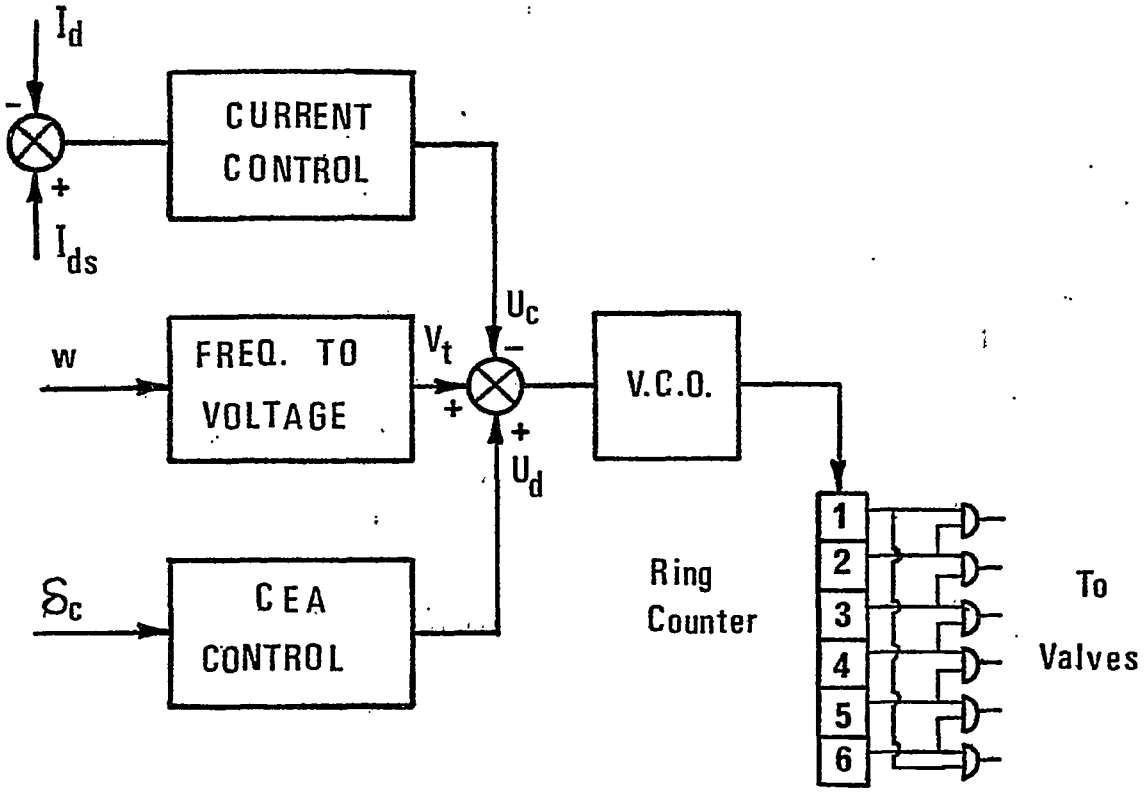

Figure 2.6 Equidistant Firing Pulse Control

CHAPTER 3

HVDC TRANSMISSION SYSTEM MODEL

The purpose of this thesis, as stated in Chapter 1, is to investigate the power-frequency interactions between AC/DC systems of the type shown in Figure 3.1. Some aspects of DC transmission have been presented in Chapter 2 for the immediate reference of the reader. It is obvious from the discussion in that chapter (Chapter 2) that, AC/DC/AC systems are complex and nonlinear, and the converters are switching devices. Two distinct approaches can be used to study the dynamic stability of these systems. One technique consists of analizing a detailed model, whereas the second method utilizes a linearized model to study small excursions in the neighbourhood of a steady state operating point. In this thesis, a small signal approach has been used to investigate various aspects of the problem already defined in Chapter 1. The model of the DC transmission system presented in this chapter has been based on the work of Burton[15,16] and Chand[17,18] except that the DC controllers used differ in some respects.

3.1 Small Signal Dynamic Model

In most cases mathematical models are derived in per unitized forms. A per unit system[19] for modelling DC transmission links normally consists of four base quantities, i.e. power, voltage, current and resistance. In these studies, the base power P_{sb} has been chosen equal to the base MVA of the AC system. Rectifier pole-to-ground no load DC voltage, U_{dro}, at the operating tap, has been selected as the base voltage. From the defined

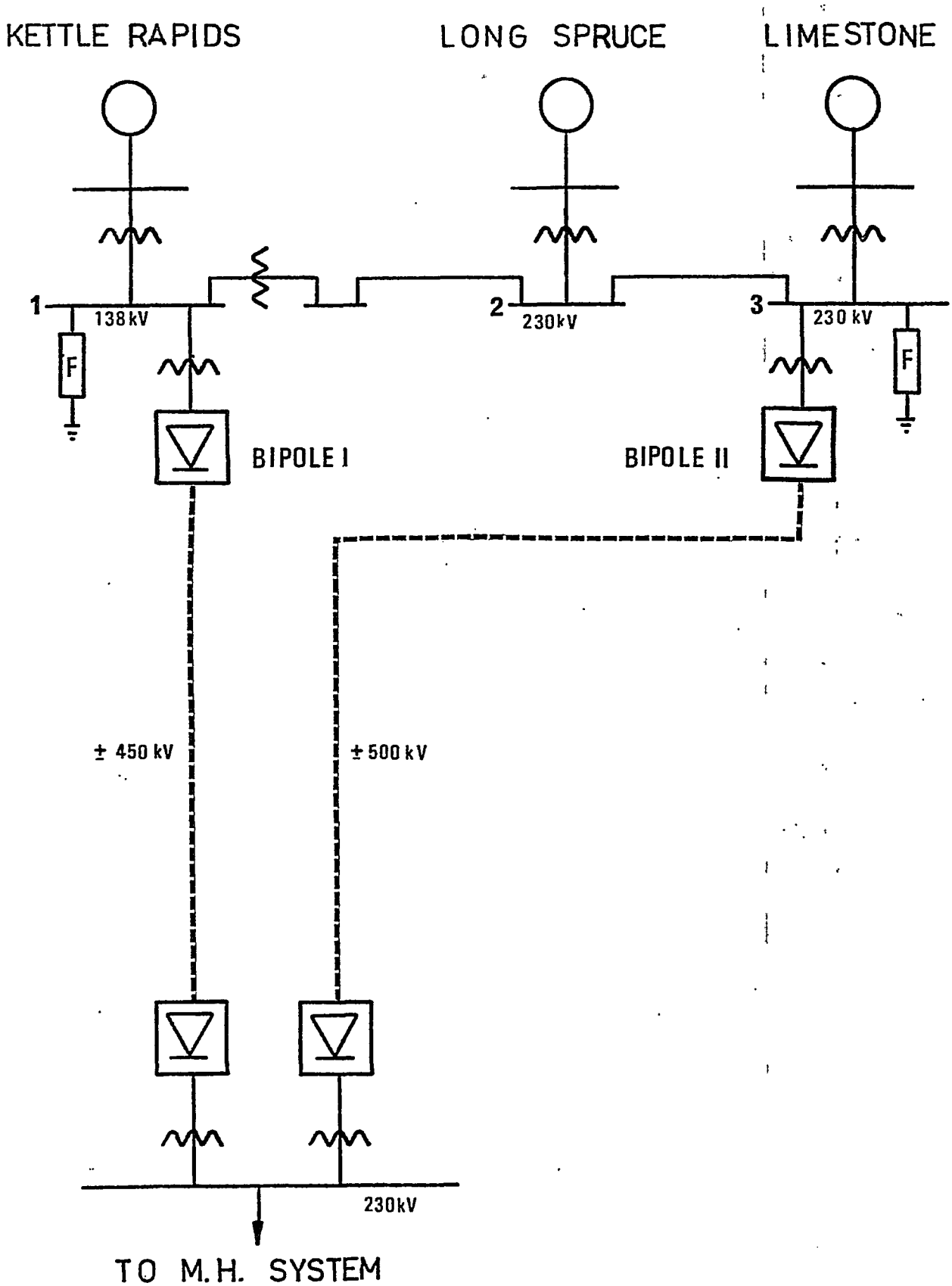

Figure 3.1 Single line diagram of the AC/DC/AC system

quantities, the remaining two base quantities are obtained as follows:

$$I_b = \frac{P_{sb}}{U_{dro}} \tag{3.1a}$$

$$R_b = \frac{(U_{dro})^2}{P_{sb}} \tag{3.1b}$$

All equations in this and subsequent chapters are given in the normalized form.

3.1.1 Converter transfer functions

The rectifier and inverter performance has been defined in Chapter 2. DC voltage of one rectifier pole of a bipolar link can be expressed as:

$$V_{dr} = \cos \alpha_r - \frac{3}{\pi} wL_r I_{dr} \tag{3.2}$$

This equation is similar to Equation 2.1, except that N_B and T_r have been absorbed in U_{dro} and L_r. Similarily, the voltage of an inverter pole can be defined as follows:

$$V_{di} = U_{dio} \cos \beta_i + \frac{3}{\pi} wL_i I_{di} \tag{3.3}$$

From Equations 3.2 and 3.3, linearized equations can be derived and are:

$$\Delta V_{dr} = \Delta e_r - \frac{3}{\pi} wL_r \Delta I_{dr} \tag{3.4}$$

$$\Delta V_{di} = \Delta e_i + \frac{3}{\pi} wL_i \Delta I_{di} \tag{3.5}$$

where: Δ denotes a small change in the associated variable;

subscript o denotes the variable at the initial operating point;

$\Delta e_r = -\sin \alpha_{ro} \Delta \alpha_r$; and

$\Delta e_i = -U_{dio} \sin \beta_{io} \Delta \beta_i$

The above equations were formulated assuming that the AC converter voltages are maintained at constant values. This assumption reduces the complexity

of the DC model and is consistant with the AC model subsequently described in this thesis.

3.1.2 Rectifier and inverter firing angle control

The small signal equations in Section 3.1.1 describe one part of the DC model only. The second part of the DC model should represent the firing angle controllers. Unfortunately, details of the controllers used in the Nelson River project are not readily available. It is assumed that an equidistant firing controller[13,15] has been used at each rectifier terminal. The linearized model of the current control loop of this controller is shown in Figure 3.2. Based on this figure, the

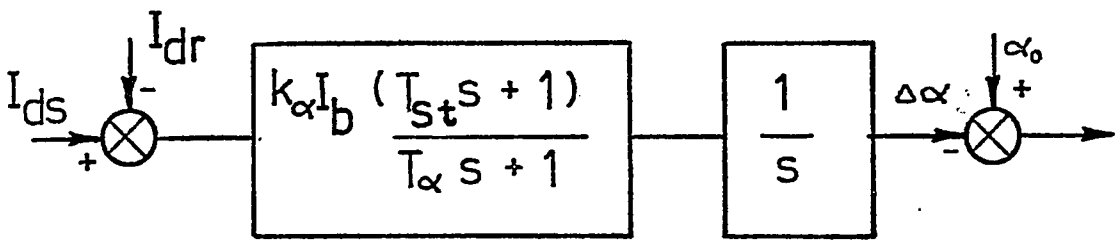

Figure 3.2 Small Signal Model of the Rectifier Current Controller

small signal equation of the rectifier current controller is:

$$\Delta\alpha_r = \frac{K_\alpha I_b (T_{st} s + 1)}{s (T_\alpha s + 1)} (\Delta I_{dr} - \Delta I_{ds}) \qquad (3.6)$$

where: I_{ds} is the current order;

α_r is the rectifier firing angle in radians;

s is the laplace operator.

At the inverter terminals, constant extinction angle controllers of the predictive type[12] are assumed to have been provided. Equation 3.7 describes this firing angle control.

$$U_{dio} \cos \beta_i - U_{dio} \cos \delta_c + \frac{6}{\pi} wL_i I_{di} = o \qquad (3.7)$$

The small signal equation representing inverter firing angle control can be expressed as follows:

$$\Delta\beta_i = \frac{1}{U_{dio} \sin \beta_{io}} \left(\frac{6}{\pi} wL_i\right) \Delta I_{di} \qquad (3.8)$$

Equations 3.6 and 3.8 describe the rectifier and inverter controllers. These equations can be combined with Equations 3.4 and 3.5 to obtain the linearized models of the inverter and rectifier terminals.

3.1.3 Transmission line model

Linearized models of AC/DC converters have been developed in Sections 3.1.1 and 3.1.2. In a DC link, the rectifier and inverter are connected by a transmission line. Therefore, a DC link model must include a suitable representation of the line connecting the converters. A DC transmission line has many natural modes of oscillation. In general, the first natural resonance is between 10 - 100 Hz.[7] The remaining resonance frequencies are much greater. Many authors have represented DC transmission lines by equivalent T models which have a frequency response close to the first natural frequency of the line. In the system studied in this thesis,

the first resonance frequency of each transmission line is about 50 Hz. The objective of this project was to investigate the power-frequency interactions which are in the 1 to 3 Hz range. Since the frequencies of interest are much smaller than the first resonance frequency of the DC line and because the first and higher order line frequencies are generally expected to be independent of the type of controller used, the transmission line can be represented by a series R-L circuit neglecting the line capacitance. Using this assumption, the transmission line performance can be expressed as follows:

$$V_{dr} = R_t I_{dr} + L_t \frac{d}{dt} (I_{dr}) + V_{di} \tag{3.9}$$

where: R_t is the total resistance of the line and the smoothing reactors;

L_t is the total inductance of the line and the smoothing reactors.

Linearizing the above equation, Equation 3.10 is obtained.

$$\Delta V_{dr} = R_t \Delta I_{dr} + L_t \frac{d}{dt} (\Delta I_{dr}) + \Delta V_{di} \tag{3.10}$$

Because of the nature of the transmission line model selected, rectifier and inverter currents are equal; that is

$$\Delta I_{dr} = \Delta I_{di} \tag{3.11}$$

Using Equations 3.4, 3.5, 3.10 and 3.11, the DC system can be represented as shown in Figure 3.3.

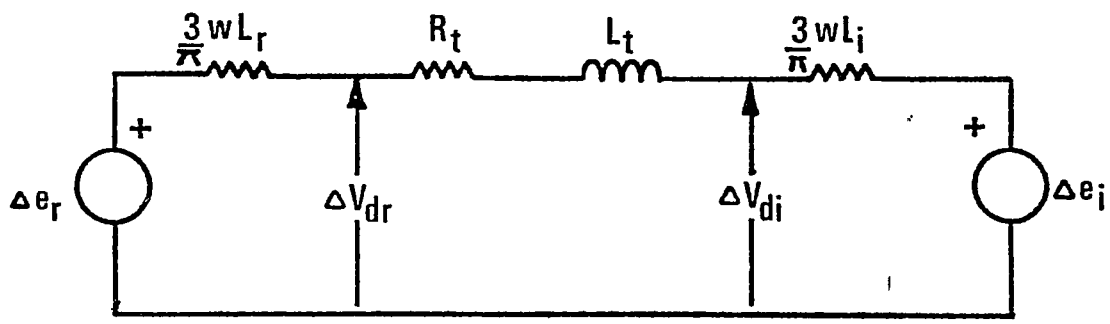

Figure 3.3 A linearized representation of the HVDC transmission system

Combining the DC model shown in Figure 3.3, with the representations of rectifier and inverter firing angle controllers (Equations 3.6 and 3.8), the rectifier and inverter voltages, and rectifier current can be defined by the following equations.

$$\Delta I_{dr} = \frac{k_{dr}(T_{st}\, s + 1)\, \Delta I_{ds}}{s^3 L_t T_\alpha + s^2(L_t + T_\alpha(R_r + R_i)) + s(k_{dr}T_{st} + R_r + R_i) + k_{dr}} \tag{3.12}$$

$$\Delta V_{dr} = \left[R_r + R_i - \frac{3}{\pi} wL_r + sL_t\right]\, \Delta I_{dr} \tag{3.13}$$

$$\Delta V_{di} = -\frac{3}{\pi} wL_i\, \Delta I_{dr} \tag{3.14}$$

where: k_{dr} is $k_\alpha I_b \sin \alpha_{ro}$;

R_r is $\frac{R_t}{2} + \frac{3}{\pi} wL_r$;

R_i is $\frac{R_t}{2} - \frac{3}{\pi} wL_i$;

s is the laplace operator.

In these equations, $\Delta\alpha_r$ and $\Delta\beta_i$ have been eliminated by algebraic manipulations. The small signal voltage and current equations, Equations 3.11 to 3.14, form the basis of the real and reactive power models which will now be presented.

3.1.4 Small signal power variations

Equations 3.11 to 3.14, given in Section 3.1.3, describe the voltage and current variations in a DC transmission system. Since the objective of this project is to investigate the power-frequency interactions between AC systems and DC links, small signal power flow equations will now be derived.

Power at the rectifier terminal of a DC transmission link is given by:

$$P_{dr} = V_{dr}\, I_{dr} \tag{3.15}$$

In small signal form, change of rectifier power can be expressed as:

$$\Delta P_{dr} = V_{dro}\, \Delta I_{dr} + I_{dro}\, \Delta V_{dr} \tag{3.16}$$

Substituting for ΔI_{dr} and ΔV_{dr} from Equations 3.12 and 3.13 respectively, Equation 3.17 is obtained.

$$\Delta P_{dr} = \frac{G_r(s + 1/T_L)\,(s + 1/T_{st})\,\Delta I_{ds}}{s^3 + s^2\left(\frac{1}{T_\alpha} + \frac{R_r + R_i}{L_t}\right) + s\left(\frac{k_{dr}T_{st} + R_r + R_i}{T_\alpha L_t}\right) + \frac{k_{dr}}{T_\alpha L_t}} \tag{3.17}$$

where: $G_r = k_{dr}\, I_{dro}\, \frac{T_{st}}{T_\alpha}$;

and $T_L = \frac{L_t}{R_r + R_i + \frac{1}{I_{dro}} \cos(\alpha_{ro} + \mu_{ro})}$. [μ_{ro} is the angle of overlap.

Equation 3.17 defines small changes in rectifier power of one pole of a DC bipolar link. Since the system to be studied consists of bipolar links, the total change in power of a DC link consisting of two identical poles can be expressed by increasing G_r by a factor of 2.

It is reasonable to select the time constant T_{st} (in Equation 3.17) to be equal to $L_t/(R_r + R_i)$, as discussed in Appendix A. This leads to a common factor of $(s + \frac{1}{T_{st}})$ in the numerator and the denominator of this equation, which can now be simplified as:

$$\Delta P_{dr} = \frac{G_r\,(s + 1/T_L)}{s^2 + D_d\, s + w_d^2}\; \Delta I_{ds} \tag{3.18}$$